Structural Basis for Substrate Binding and the Catalytic Mechanism of Type III Pantothenate Kinase †

ARTICLE *in* BIOCHEMISTRY · MARCH 2008

Impact Factor: 3.02 · DOI: 10.1021/bi7018578 · Source: PubMed

4 AUTHORS, INCLUDING:

Erick Strauss
Stellenbosch University
38 PUBLICATIONS **868** CITATIONS
SEE PROFILE

Hong Zhang
University of Texas Southwestern Medical Ce…
34 PUBLICATIONS **1,041** CITATIONS
SEE PROFILE

Structural Basis for Substrate Binding and the Catalytic Mechanism of Type III Pantothenate Kinase†

Kun Yang,‡ Erick Strauss,§ Carlos Huerta,‡ and Hong Zhang*,‡

Department of Biochemistry, University of Texas Southwestern Medical Center, Dallas, Texas 75390, and Department of Chemistry, Stellenbosch University, Matieland 7602, South Africa

Received September 11, 2007; Revised Manuscript Received November 26, 2007

ABSTRACT: Pantothenate kinase (PanK) catalyzes the first step of the universal five-step coenzyme A (CoA) biosynthetic pathway. The recently characterized type III PanK (PanK-III, encoded by the *coaX* gene) is distinct in sequence, structure and enzymatic properties from both the long-known bacterial type I PanK (PanK-I, exemplified by the *Escherichia coli* CoaA protein) and the predominantly eukaryotic type II PanK (PanK-II). PanK-III enzymes have an unusually high K_m for ATP, are resistant to feedback inhibition by CoA, and are unable to utilize the *N*-alkylpantothenamide family of pantothenate analogues as alternative substrates, thus making type III PanK ineffective in generating CoA analogues as antimetabolites *in vivo*. Previously, we reported the crystal structure of the PanK-III from *Thermotoga maritima* and identified it as a member of the "acetate and sugar kinase/heat shock protein 70/actin" (ASKHA) superfamily. Here we report the crystal structures of the same PanK-III in complex with one of its substrates (pantothenate), its product (phosphopantothenate) as well as a ternary complex structure of PanK-III with pantothenate and ADP. These results are combined with isothermal titration calorimetry experiments to present a detailed structural and thermodynamic characterization of the interactions between PanK-III and its substrates ATP and pantothenate. Comparison of substrate binding and catalytic sites of PanK-III with that of eukaryotic PanK-II revealed drastic differences in the binding modes for both ATP and pantothenate substrates, and suggests that these differences may be exploited in the development of new inhibitors specifically targeting PanK-III.

Coenzyme A (CoA[1]) is a ubiquitous and essential cofactor in all living organisms where it functions as the major acyl group carrier in many crucial cellular processes, most notably in the tricarboxylic acid (TCA) cycle and in fatty acid metabolism. Pantothenate kinase (PanK) catalyzes the first and rate-limiting step in the universal five-step CoA biosynthetic pathway, transferring a phosphoryl group from ATP to pantothenate (Pan) (*1*−*3*) (Scheme 1). The essential requirement of CoA, in combination with the fact that it has to be biosynthesized *de novo* from pantothenate in all organisms, has led to the recognition of CoA biosynthetic enzymes as possible new antimicrobial targets of important human pathogens (*4*, *5*). In this regard inhibitors that specifically target PanK are of special interest due to the enzyme's key role in regulating the intracellular concentration of CoA and the lack of homology between bacterial PanK enzymes and their human counterparts, and their development is actively being pursued (*6*−*8*).

Three distinct types of PanK have been characterized thus far: the type I PanK (PanK-I), exemplified by *Escherichia coli* CoaA protein, was originally thought to represent the majority of PanK enzymes from prokaryotic sources. Type II PanKs (PanK-II), in contrast, predominantly occur in eukaryotic organisms. These two types of PanK have long been the subject of intensive investigations (*9*−*14*). These studies have shown that although they are evolutionarily unrelated, both types are feedback inhibited by the end-product of the pathway in the form of either CoA or its thioesters, and thus play a key regulatory role in CoA biosynthesis and homeostasis in the cell (*12*, *13*, *15*−*17*). Furthermore, both PanK-I and PanK-II enzymes are able to phosphorylate a class of pantothenate analogues known as the *N*-alkylpantothenamides, allowing them to be transformed by the organism's native CoA biosynthetic pathway into inactive CoA analogues which act as antimetabolites and effective inhibitors of bacterial growth (*6*, *7*, *18*). Interestingly, the distinction between these two types of PanK cannot be made solely based on phylogenetic relationships, as "eukaryotic" PanK-II-like enzymes are also found in a few

† This work was supported by NIH Grant GM63689 and a Welch Foundation Grant (I-1505). E.S. is supported by grants from the National Research Foundation of South Africa (FA2005040600033) and Stellenbosch University. Use of Argonne National Laboratory Structure Biology Center beamline at Advanced Photon source was supported by the U.S. Department of Energy, Office of Biological and Environmental Research, under Contract No. W-31-109-ENG-38.

* Corresponding author. E-mail: zhang@chop.swmed.edu. Phone: 214-645-6372. Fax: 214-645-5948.

‡ University of Texas Southwestern Medical Center.

§ Stellenbosch University.

[1] Abbreviations: ASKHA, acetate and sugar kinase/heat shock protein 70/actin; CoA, coenzyme A; Pan, pantothenate; P-Pan, phosphopantothenate; PanK, pantothenate kinase; ITC, isothermal calorimetry; AMPPNP, 5′-adenylyl-β,γ-imidodiphosphate; PEP, phosphoenolpyruvate; NTP, nucleoside triphosphate; dNTP, deoxynucleoside triphosphate; rmsd, root mean square deviation; HEPES, 4-(2-hydroxyethyl)-1-piperazineethanesulfonic acid; DTT, dithiothreitol; PEG, polyethylene glycol; *Ba, Bacillus anthracis; Bs, Bacillus subtilis; Tm, Thermotoga maritima; Hp, Helicobacter pylori; Mt, Mycobacterium tuberculosis; Pa, Pseudomonas aeruginosa.*

10.1021/bi7018578 CCC: $40.75
Published on Web 01/11/2008

Scheme 1

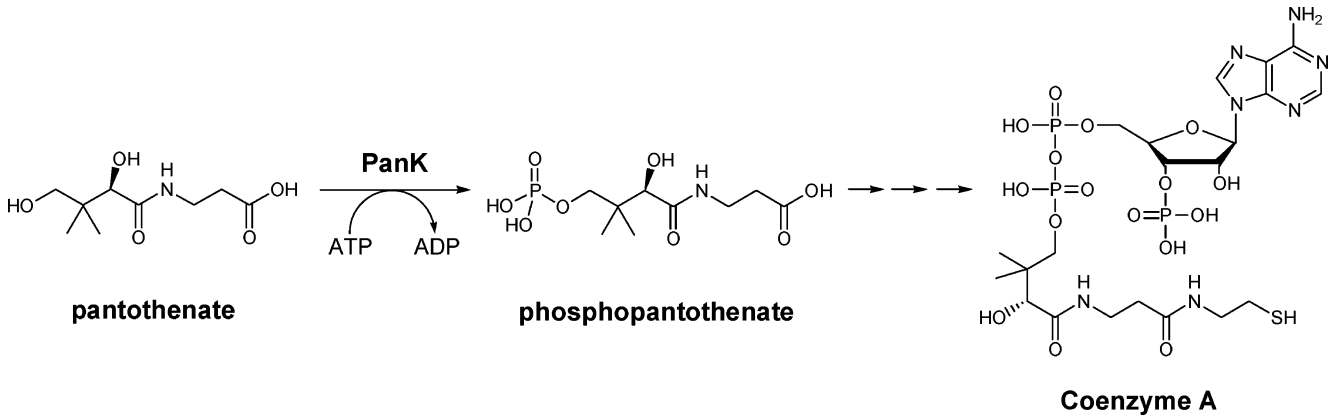

Gram-positive bacteria, most notably *Bacillus anthracis* and *Staphylococcus aureus* (*7*, *19*, *20*). These bacterial PanK-II enzymes share significant sequence and structural similarity with their eukaryotic counterparts, although they do exhibit differences in certain catalytic properties (*7*, *21*, *22*). In particular, PanK-II from *S. aureus* (*Sa*PanK-II) is not subject to inhibition by either CoA or its thioesters (*21*), a property that is most likely related to the additional metabolic function of CoA as the major low molecular weight thiol in this organism, which uses CoA and an NADPH-dependent CoA disulfide reductase to maintain its redox balance (*19*, *23*, *24*).

Recently a third type of PanK (PanK-III, encoded by the gene denoted as *coaX*, to be distinguished from *coaA*) was identified in bacteria (*25*, *26*). A comprehensive analysis of the PanK-encoding genes in more than 300 complete or nearly complete bacterial genomes using THE SEED tool (http://theseed.uchicago.edu/FIG/index.cgi) (*27*) revealed that PanK-III enzymes have a much wider phylogenetic distribution than the better known PanK-I, being present in 12 of the 13 major bacterial groups, and in many pathogenic bacteria (*20*). PanK-I, in contrast, is present in only four of these groups. Recent studies of the biochemical properties of PanK-III enzymes from several bacterial species have shown that PanK-III differs significantly from both PanK-I and PanK-II as PanK-III enzymes are not feedback inhibited by CoA, and cannot use *N*-alkylpantothenamides as substrates (*20*, *22*, *25*). Additionally, PanK-III has an unusually high K_m for ATP (in the millimolar range) and requires a monovalent cation for catalysis (*22*, *25*).

From a structural perspective, it has long been known that bacterial type I PanKs belong to the P-loop kinase superfamily based on both sequence and structural evidence (*15*, *28*). More recently, structures of type II and type III PanKs were also determined (*19*, *20*, *22*, *29*). These structures confirmed a previous prediction that both PanK-II and PanK-III are evolutionarily unrelated to PanK-I, adopting an actin-like fold instead—this places them in the ASKHA (an abbreviation for "acetate and sugar kinase/Hsp70/actin") protein superfamily (*30*, *31*). However, notwithstanding their shared common fold and conserved key catalytic residues, PanK-II and PanK-III appear to differ significantly in dimer formation and in the detailed substrate binding site configurations that underlie their different enzymatic properties (*22*). These differences would be particularly relevant to any effort directed at the development of inhibitors targeting PanK-III.

To further aid our efforts in this regard we report here the crystal structures of PanK-III from *Thermotoga maritima* (*Tm*PanK-III) in complex with its substrate (i.e., pantothenate), product (phosphopantothenate), or both pantothenate and ADP. These structures, in combination with isothermal titration calorimetry (ITC) analysis of the binding of the substrates to the protein, provide a detailed picture of the interactions between both the substrates and the enzyme while shedding new light onto the unique kinetic properties of PanK-III. Our results further highlight the drastic differences in the substrate binding sites of type II and type III PanKs, which should facilitate the structure based approach for developing inhibitors specifically targeting PanK-III enzymes.

EXPERIMENTAL PROCEDURES

Isothermal Titration Calorimetry (ITC). PanK-III from *T. maritima* and *Helicobacter pylori* (*Tm*PanK-III and *Hp*PanK-III) were cloned, expressed, and purified as described before (*20*, *25*). In preparation for the isothermal calorimetric (ITC) assays, proteins were exhaustively exchanged into a buffer containing 100 mM NaCl, 20 mM Tris, pH 8.0. Protein concentrations were determined by measuring the absorbance at 280 nm and were calculated according to Beer's law using extinction coefficients obtained from the ProtParam tool available at the ExPASy Proteomics Sever (www.Expasy-.org). The extinction coefficients that were used are 27055 $M^{-1}\cdot cm^{-1}$ and 13910 $M^{-1}\cdot cm^{-1}$ for *Tm*PanK-III and *Hp*-PanK-III, respectively. The protein concentrations were further confirmed using the Bradford assay (*32*) with bovine serum albumin (Sigma, St. Louis, MO) as a standard. The calorimetric titration experiments were carried out at 20 °C in a VP-ITC titration microcalorimeter (MicroCal, Northampton, MA). Ligand at a stock concentration of 1 mM (for pantothenate) or 4 mM (for ATP or AMPPNP) was titrated into a sample cell (1.4 mL) containing PanK-III proteins at a concentration of 0.1 or 0.28 mM, respectively. Nucleotides were used at a higher concentration along with a higher concentration of proteins in order to increase the observed signals of small heat changes associated with nucleotide binding. The heat change from protein−ligand interaction was monitored by the VP-ITC instrument until the target protein was saturated with the ligands. Data were processed and fitted using Microcal ORIGIN software (OriginLab, Northampton, MA).

Table 1: Data Collection and Refinement Statistics

	*Tm*PanK·Pan binary complex	*Tm*PanK·P-Pan binary complex	*Tm*PanK·Pan·ADP ternary complex
data collection			
wavelength (Å)	0.9790	0.9790	1.5418
resolution (Å)	50−1.51	50−1.63	50−2.30
total no. of observations	855,017	686,415	255,007
no. of unique reflections	220,185	176,024	62,103
completeness (% in outer shell)	99.7 (98.4)	99.4 (94.0)	98.9 (97.6)
R_{sym} (outer shell)[a]	0.061 (0.361)	0.057 (0.356)	0.066 (0.251)
I/σ (outer shell)	11.3 (5.0)	18.9 (9.2)	44 (7.9)
refinement			
R_{work}[b]	0.184	0.185	0.190
R_{free}[c]	0.213	0.229	0.257
protein atoms (av *B*-factor, Å^2)	11574 (19.3)	11528 (20.3)	11574 (20.9)
solvent atoms (av *B*-factor, Å^2)	1807 (34.1)	1652 (34.2)	648 (23.9)
Pan atoms (av *B*-factor, Å^2)	15 (13.7)		15 (14.5)
P-pan atoms (av *B*-factor, Å^2)		19 (19.0)	
ADP atoms (av *B*-factor, Å^2)			27 (43.4)
rmsd bond length (Å)	0.009	0.010	0.009
rmsd bond angle (deg)	1.37	1.49	1.41
Ramachandran plot			
% in most favored region	92.0	92.5	92.5
% in additional allowed region	8.0	7.4	7.5
% in disallowed region	0	0.1	0.1

[a] $R_{sym} = \sum_{hkl}\sum_j|I_j - \langle I\rangle|/\sum_{hkl}\sum_j|I_j|$. [b] $R_{work} = \sum_{hkl}|F_o - F_c|/\sum_{hkl}|F_o|$, where F_o and F_c are the observed and calculated structure factors, respectively. [c] Five percent randomly selected reflections were excluded from the refinement and used in the calculation of R_{free}.

Enzyme Activity and Kinetic Assays. The enzyme activity assay and steady-state kinetics were carried out as described before (*25*) with minor modifications. Briefly, a continuous spectrophotometric assay that couples the production of ADP to the reactions catalyzed by pyruvate kinase and lactate dehydrogenase was used and the consumption of NADH was monitored by changes in absorption at 340 nm. Each 600 μL reaction mixture contained 100 mM HEPES, pH 7.6, 20 mM KCl, 10 mM $MgCl_2$, 2 mM phosphoenolpyruvate (PEP), 0.3 mM NADH, 5 units of lactate dehydrogenase, 2.5 units of pyruvate kinase and an appropriate amount of pantothenate and ATP. The concentration of pantothenate was varied from 5 to 80 μM while the ATP concentration varied between 2 and 20 mM. The reactions were initiated by the addition of the reaction mixture to the PanK-III protein (final concentration 0.27 μM) placed in cuvettes. Apparent K_m (for pantothenate) and k_{cat} values were calculated by fitting initial rates to a standard Michaelis−Menten model using the SigmaPlot software package. The plot of velocity versus ATP concentration has a sigmoidal appearance and was fitted to the Hill equation $(v/V_{max}) = [ATP]^n/(K' + [ATP]^n)$ to determine the kinetic parameters for ATP.

Crystallization, Data Collection, and Refinement. Cocrystals of *Thermotoga maritima* PanK (*Tm*PanK) complexes were grown using the hanging drop vapor-diffusion method in conditions similar to that of the native proteins (*20*). Prior to crystallization, 20 mg/mL *Tm*PanK protein, in 20 mM HEPES, pH 8.0, 200 mM NaCl and 1 mM DTT, was incubated with either 5 mM pantothenic acid (Pan), 5 mM phosphopantothenate (P-Pan, synthesized as described previously (*33*, *34*)), or both 5 mM pantothenic acid and 30 mM ADP for the growth of binary and ternary complexes. The complex solution (1.5 μL) was then mixed with an equal volume of the reservoir solution containing 16% PEG-3350, and was allowed to equilibrate against the same reservoir over a period of several days at 4 °C. Diffraction data for the ternary complex (*Tm*PanK-III·Pan·ADP) was collected in-house on an RAXIS-IV^{++} image plate detector equipped with a Rigaku FR-E SuperBright X-ray generator and Osmic Varimax HF mirrors. Data from two binary complex crystals, *Tm*PanK-III·Pan and *Tm*PanK-III·P-Pan, were collected at beamline 19-BM at the Advance Photon Source, Argonne National Laboratory (Argonne, IL). The diffraction data were indexed, integrated, and scaled using the HKL2000 program package (*35*). The crystals of *Tm*PanK-III·Pan and *Tm*PanK-III·Pan·ADP complexes are isomorphous to the uncomplexed crystal and belong to the space group $P2_1$, with unit cell dimensions $a = 74.92$ Å, $b = 136.99$ Å, $c = 74.97$ Å, and $\beta = 109.62°$. The product complex crystals, though also of the same space group with similar unit cell dimensions, have different crystal packing interactions. Therefore the molecular replacement method as implemented in the MOLREP (*36*) program was used to solve the initial phases of *Tm*PanK-III·P-Pan complex structure.

Refinement and model building of all three *Tm*PanK-III complexes were carried out using the Refmac (*37*) program in the CCP4 package (*38*) and Coot (*39*). After a first round of refinement, the $F_o - F_c$ difference electron density maps revealed clear density for the bound ligands. These ligand molecules, Pan, ADP, and P-Pan, were built in the model based on the difference densities. The solvent molecules were added subsequently using Coot (*39*). The program PROCHECK (*40*) was used to evaluate the quality of the structures. The data collection and final refinement statistics are given in Table 1. All figures were made using PyMOL (*41*).

Protein Structure Accession Numbers. Coordinates of *Tm*PanK-III·Pan, *Tm*PanK-III·Pan·ADP, and *Tm*PanK-III·P-Pan have been deposited in the Research Collaboratory for Structural Bioinformatics (RCSB) Protein Data Bank (*42*) under accession codes 3BEX, 3BF1, and 3BF3, respectively.

RESULTS AND DISCUSSION

Thermodynamic Characterization of Interactions between PanK-III and Its Substrates. One of the unusual enzymatic properties of PanK-III is its high K_m value for ATP (~3−10 mM) (*20*, *22*, *25*). Experiments done with PanK-III from *H. pylori* and *P. aeruginosa* (*Hp*PanK-III and *Pa*PanK-III) have excluded several alternative phosphoryl donors such as phosphoenolpyruvate, acetyl- and carbamoylphosphate as possible substrates of PanK-III. It has also been shown that although PanK-III enzymes are able to utilize various different NTPs and dNTPs as phosphoryl donors, they exhibit a trend which indicates that the purine nucleotides (ATP, GTP, dATP and dGTP) are slightly more efficient as substrates than pyrimidine nucleotides. Nonetheless, their activities are generally the highest when using ATP as the substrate (*22*).

To gain further insight into the nature of the enzyme−substrate interactions and to obtain unbiased binding affinities of each substrate (Pan or ATP) toward PanK-III, we carried out isothermal titration calorimetry (ITC) experiments with two divergent PanK-III enzymes from *Thermotoga maritima* and *Helicobacter pylori*, respectively. Our results show that pantothenate binds to both PanK-III enzymes with high affinity (Figure 1), with $K_{d,Pan}$ ranging from 2.7 to 6.4 μM (Table 2). Interestingly, the titration profile revealed that the two pantothenate binding sites of the *Tm*PanK-III dimer do not appear to be the same under the assay conditions, as the data agree the best with a sequential two-site model with the first site having a K_d of 2.7 μM, and the second 6.4 μM. This result suggests a slightly negative cooperativity between the two pantothenate binding sites in the *Tm*PanK-III dimer. No cooperativity is observed between the two pantothenate binding sites of *Hp*PanK-III dimer, where the two sites appear to act independently of each other (Figure 1). The same lack of cooperativity in Pan-binding was also observed in *P. aeruginosa* PanK-III (data not shown). Therefore the slight negative cooperativity of Pan-binding in *Tm*PanK-III does not appear to be a prevalent feature of the family.

The negative enthalpy changes for the binding of pantothenate to both PanK-III enzymes (Table 2) indicate that the reaction is exothermic and there is an overall increase in interactions between Pan and the enzyme. The entropy changes (ΔS) for pantothenate binding were small for *Hp*PanK-III and for site 1 of the *Tm*PanK-III dimer, but increased to a larger negative value (~−3 cal/mol/deg) for site 2 of *Tm*PanK-III. It would thus appear that there are enhanced hydrogen bonding and hydrophobic interactions between Pan and protein at site 2 of *Tm*PanK-III, resulting in an increase in order and consequently in a more negative ΔS. All of these observations are consistent with extensive enzyme−pantothenate interactions that include both specific hydrogen bonds and hydrophobic interactions as observed in the PanK-III·Pan complex structures (see (*22*) and the discussion below). In contrast, the binding of either ATP or the ATP analogue AMPPNP to PanK-III is endothermic, and is accompanied by a more favorable entropy component (Table 2). Overall the favorable entropy contribution is sufficient to offset the unfavorable enthalpic changes, and the free energy change ΔG for ATP binding is consequently negative (Table 2).

To establish whether there is any synergism or antagonism in the binding of the substrates (ATP and pantothenate) of PanK-III we also determined the binding constants of the *T. maritima* and *H. pylori* enzymes for both pantothenate and the ATP analogue AMPPNP in the presence of the other substrate. The results show that the binding affinities of pantothenate and ATP analogue in the presence and absence of the second substrate are essentially identical (data not shown), suggesting that the Pan and ATP binding occurs independently of each other. This is in contrast to the strong synergism observed for substrate binding in hexokinase, another member of the ASKHA superfamily, where binding of the sugar molecule causes significant conformational changes in enzyme active site which greatly facilitate the subsequent binding of MgATP (*43*−*45*).

Steady-State Kinetic Parameters of HpPanK-III. The K_d values for pantothenate (~3−6 μM) obtained in the ITC assays are quite different from the previously determined $K_{m,Pan}$ values for *Hp*PanK-III, which was in the ~100 μM range (*25*). To investigate the basis for this difference we revisited the steady-state kinetic experiments. Care was taken to ensure that data were collected during the initial rate phase of the reaction (<10% substrate consumed) (see Experimental Procedures). Under these conditions the apparent $K_{m,Pan}$ was determined to be 5.5 μM for *Hp*PanK-III (Figure 2A), which is essentially the same as the K_d value of Pan determined with the ITC experiment (5.6 μM). The plot of velocity versus ATP concentration has a sigmoidal appearance suggesting cooperative binding of ATP by *Hp*PanK-III (Figure 2B). The data was thus fitted to the Hill equation, and a $K' = 62$ mM and $n = 2.0$ was obtained. This yielded an apparent K_m for ATP of 7.9 mM, similar to the previously determined value of 9.6 mM. Since *Hp*PanK-III exists in solution as a dimer (data not shown), this observation may suggest a strong cooperativity between the two ATP binding sites of *Hp*PanK-III dimer. Since the *Hp*PanK-III structure has not yet been determined, the basis for this cooperativity is not clear. It thus remains to be seen whether this is a shared property among other members of PanK-III enzymes. Although data from the ITC experiments suggest that the binding of ATP and pantothenate is independent of each other, we have observed significant substrate inhibition (~25%) by ATP when the ATP concentration is increased to 20 mM. This observation is consistent with the notion that pantothenate probably prefers to bind to PanK-III before ATP, as based on structural considerations (*22*). The apparent independence in the binding of the substrates to PanK-III is most likely due to the extreme disparity in binding affinities (~500-fold) of the two substrates.

The nearly identical values of K_d obtained from the ITC assays and the K_m from the steady-state kinetic analyses suggest that substrate binding rather than catalysis is likely the rate-limiting step of the enzyme. As PanK-III enzymes are not regulated through feedback inhibition by CoA (the end product of the pathway), its relatively high affinity for pantothenate and low affinity for ATP may be of important physiological consequence for CoA biosynthesis and homeostasis in organisms harboring type III PanK enzymes.

The Overall Structures of the TmPanK-III Complexes. Previously, the structures of the PanK-III enzymes from *T. maritima* and *B. anthracis* in their apo forms and the structures of PanK-III from *P. aeruginosa* in both apo- and

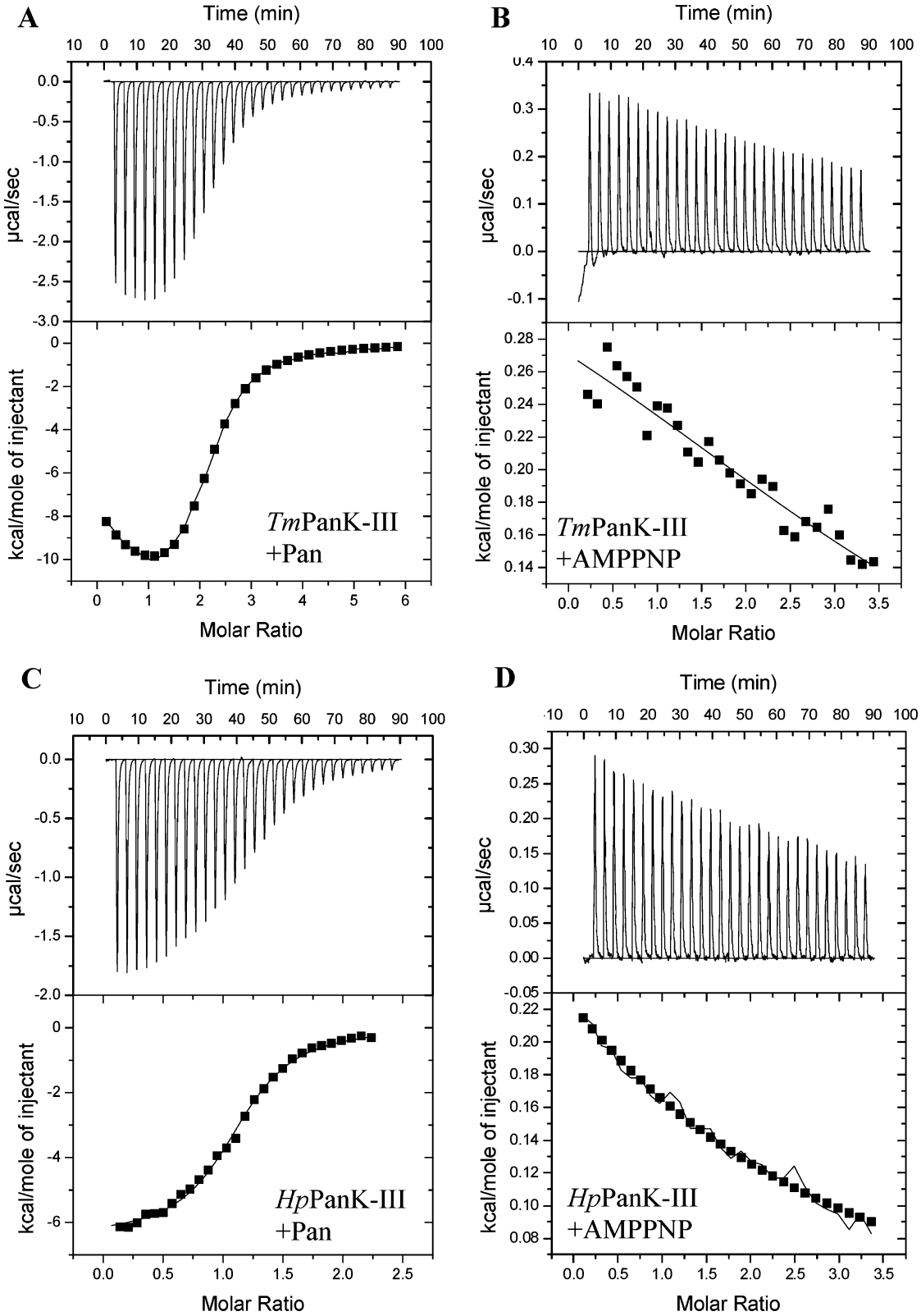

FIGURE 1: Calorimetric titrations of PanK-III enzymes with pantothenate (A and C) and AMPPNP (B and D). The results obtained from titrations of ATP are not shown, but were essentially identical to those obtained with AMPPNP. The upper panel in each graph shows the heat changes elicited by successive injections of respective ligand into *Tm*PanK-III (A and B) or *Hp*PanK-III (C and D). The lower panels show the binding isotherms as a function of the molar ratio of ligand to enzyme. The theoretical curves were fitted to the integrated data. A sequential two-site model was used in A, while a one-site binding model was used in B, C, and D. Note the difference scales used in each graph.

pantothenate-bound forms were reported (*19*, *20*, *22*). We have now also obtained crystal structures of two binary complexes of *Tm*PanK-III with its substrate (pantothenate) and product (phosphopantothenate), respectively, as well as a ternary complex *Tm*PanK-III·Pan·ADP (Figure 3A). The overall structures of these complexes are very similar to that of the apo enzyme (*20*), with an average root-mean-square deviation (rmsd) between C_α positions of ~0.3 Å. There

Table 2: Thermodynamic Parameters of Interactions between Substrate and PanK-III

		Pan				AMPPNP			
		K_d (μM)	ΔH (kcal/M)	$T\Delta S$ (kcal/M)	ΔG (kcal/M)	K_d (mM)	ΔH (kcal/M)	$T\Delta S$ (kcal/M)	ΔG (kcal/M)
*Tm*PanK-III	site 1	2.7 ± 0.16	-8.4 ± 0.07	-0.94	-7.5	3.0 ± 0.50	2.9 ± 0.36	6.2	-3.3
	site 2	6.4 ± 0.24	-15.2 ± 0.11	-8.20	-7.0				
*Hp*PanK-III		5.6 ± 0.34	-6.4 ± 0.06	0.59	-7.0	2.3 ± 0.15	2.0 ± 0.10	5.6	-3.4

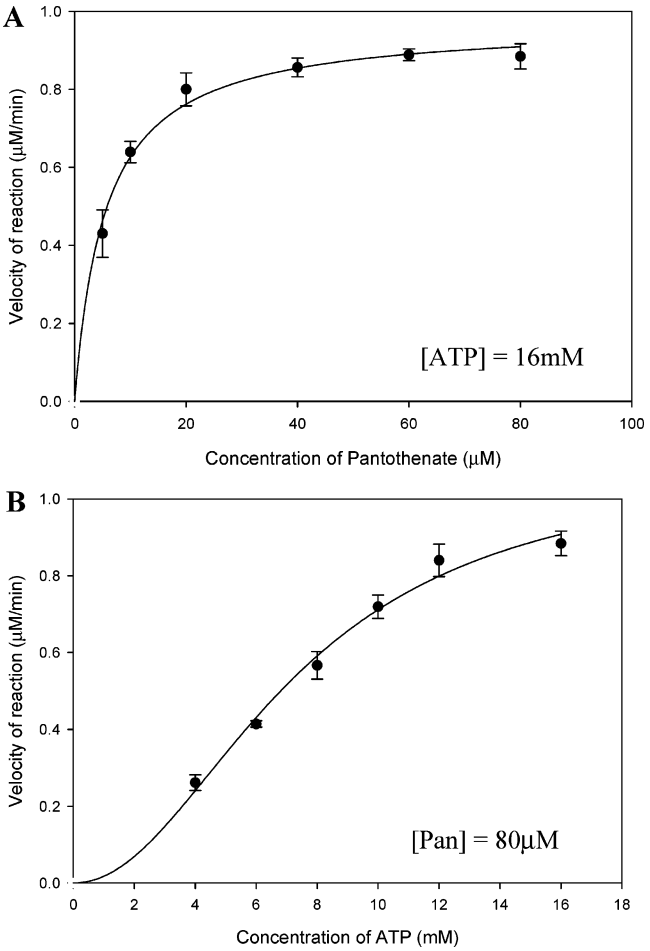

FIGURE 2: Plots of initial rate (v) versus pantothenate (A) and ATP concentrations (B) for *Hp*PanK-III. The v versus [Pan] data is fitted to the Michaelis−Menten equation (A), while the v versus [ATP] data is fitted to the Hill equation (B) (see Experimental Procedures). Each data point is the average of four measurements.

appears to be no significant conformational differences in *Tm*PanK-III complexes compared to the apoenzyme under the crystallization conditions.

The structure of *Tm*PanK-III is also similar to that of PanK-III from *P. aeruginosa* (*Pa*PanK-III) (*22*). The two enzymes share ~23% sequence identity, and the rmsd between their C_α atoms is 1.8 Å. In contrast, CoaA from *S. aureus*, a type-II PanK (*Sa*PanK-II) which also belongs to the ASHKA protein superfamily, is much more divergent from PanK-III, with a large rmsd (2.9 Å) over ~180 superimposed C_α atoms and a sequence identity of only 13%. PanK-II and PanK-III share a common fold generally referred to as an "actin-like" or "ribonuclease H-like" fold that contains a duplication of two domains with each domain consisting of a five-stranded mixed β-sheet and three flanking α helices (*30*, *31*). The substrate binding and catalytic site is located at the interface between the two domains (Figure 3A). The signature motifs of the superfamily including ADENOSINE, PHOSPHATE 1 and PHOSPHATE 2 are conserved in both PanK-II and PanK-III (*19*, *20*, *22*, *30*) (Figure 3B). However, there are significant differences in the peripheral structural elements and in the relative arrangement of the monomers in the dimer, which result in substantially different substrate binding modes (see below).

Pantothenate Binding Site. In the *Tm*PanK-III·Pan complex as well as the ternary *Tm*PanK-III·Pan·ADP complex structures the conformation of the bound pantothenate molecule is well-defined by the unambiguous electron densities (Figure 4A). The bound pantothenate is located in a small cavity at the domain interface and forms extensive and highly specific interactions with protein residues from both monomers of the *Tm*PanK-III dimer (Figure 4B). Two structural motifs unique to PanK-III form the rest of the largely enclosed Pan binding pocket. The first is the "Pan Cap" loop from the second monomer of the dimer (residues 158−165) (*20*). This loop is part of the highly variable insertion element in the C-terminal domain and tends to be flexible or even disordered in the absence of substrate in cases of the PanK-III enzymes from *P. aeruginosa* and *B. anthracis*, but becomes ordered upon binding of pantothenate (*19*, *22*). The second PanK-III specific motif was named the "Pan motif" by Nicely et al. (*19*) and comprises an extended loop connecting the last β-strand of the N-terminal domain (β5) to α3 helix, and also includes the highly conserved residues Asp105 and Arg106 (Figure 3, 4B). This loop is another unique insertion element to the ASKHA core of PanK-III and is not present in PanK-II. Most specific interactions between the enzyme and Pan are formed through residues from these two motifs. At one end of the Pan molecule, the C1 carboxyl group forms two hydrogen bonds with the side chains of Arg106 and $Thr179_B$ (the subscript "B" denotes residues from the second monomer), while at the other end the C2′ and the C4′ hydroxyl groups are hydrogen bonded to the side chain of Asp105. The carbonyl oxygen of Pan interacts with Asn9 indirectly through a water molecule; and the 3′ geminal dimethyl groups make van der Waals contact with the side chains of Ile145 and $Leu163_B$. Together the two Pan-binding motifs complete the enclosed Pan-binding pocket of PanK-III (Figures 3A and 4B).

Superimposition of the pantothenate binding pocket of *Tm*PanK-III with that of *Pa*PanK-III reveals that the position and conformation of Pan in the two structures are essentially identical (Figure 5). Most of the Pan-interacting residues are conserved in both enzymes. These include Asn9, Asp105, Arg106, Ile145, $Leu163_B$ and $Thr179_B$ of *Tm*PanK-III, corresponding to Asn9, Asp101, Arg102, Ile142, $Ile160_B$, and $Thr180_B$ of *Pa*PanK-III, respectively. A notable difference in Pan-binding sites of the two enzymes is the presence of Tyr92 in *Pa*PanK-III, which forms a hydrogen bond to the carboxylate group of Pan. This tyrosine residue is also

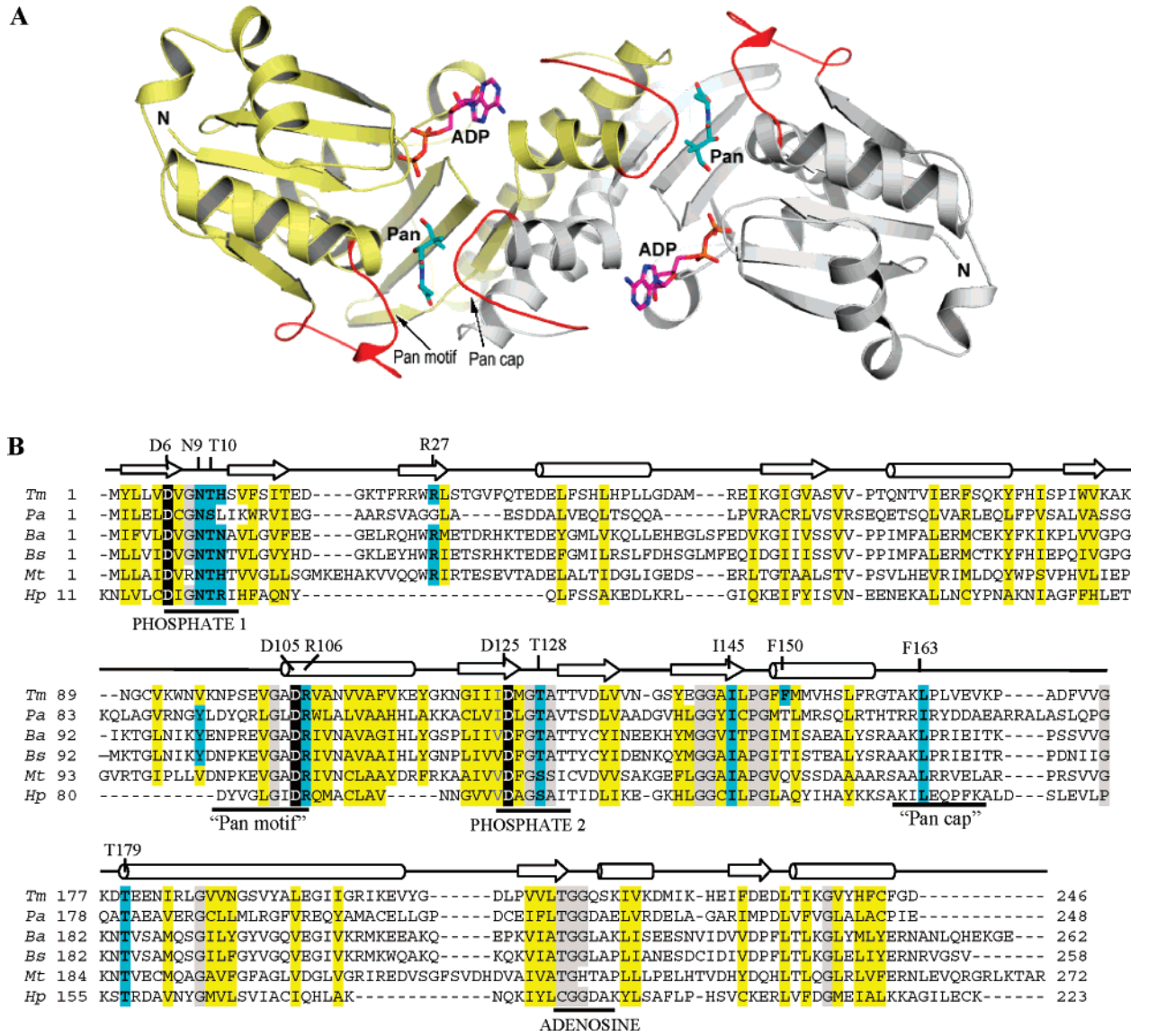

FIGURE 3: (A) The ribbon diagram of *Tm*PanK-III dimer with bound ADP and Pan. The two PanK-III specific motifs ("Pan cap" and "Pan motif") are highlighted in red. (B) Multiple sequence alignment of selected PanK-III sequences including those with available 3D structures. Secondary structure elements are indicated at the top with arrows representing β-strands and cylinders representing α-helices. The conserved motifs within the ASKHA superfamily (PHOSPHATE 1, PHOSPHATE 2 and ADENOSINE) and those specific for PanK-III ("pan motif" and "pan cap") are underlined. Residues that interact with bound substrates are shaded in cyan, and indicated on top of the secondary structure cartoon (using *Tm*PanK-III numbering). The generally conserved hydrophobic or neutral residues are shaded in yellow, while conserved small residues (G, P, S, A, T) are shaded in gray.

present in the enzymes from *Bacillus* species (Figure 3B), corresponding to Tyr100 of *Ba*PanK-III, but is changed to a Val residue (Val96) in other PanK-III enzymes such as those from *T. maritima* and *M. tuberculosis* (Figure 3B). Nevertheless, given the high degrees of conservation of most residues interacting with pantothenate and similar Pan-binding affinities observed among divergent members of PanK-III enzymes, it is likely that the general Pan-binding mode is highly conserved in all type III PanKs.

ATP Binding Site. Despite a very low affinity between PanK-III and nucleotide ($K_d \sim 3$ mM), we were able to obtain a *Tm*PanK-III·Pan·ADP ternary complex structure, which offered a first view of the interactions between the nucleotide and enzyme. Notably, the *B*-factors of the bound ADP molecule are higher than that of surrounding protein atoms (43 Å^2 vs 20 Å^2), indicating partial occupancy or disordering. Nevertheless the electron density for ADP is clear enough to allow unambiguous assignment of the adenine base, ribose and the two phosphate groups (Figure 4A).

The ADP molecule binds in a cleft between the two domains of the enzyme (Figures 3, 4), in a position generally conserved for nucleotide binding in the ASKHA superfamily (*28*, *31*, *46*). Most interactions between ADP and the enzyme are formed through the two phosphate groups of ADP. Here the α-phosphate of the bound ADP forms several hydrogen bonds with the enzyme, specifically through direct interaction with the side chains of Thr10, His11 (both are part of the "PHOSPHATE 1" motif) and Arg27. The β-phosphate of ADP is hydrogen bonded to the side chains of Thr10 and Thr128 directly, and indirectly to Asp6 and Asn9 through water molecules. The β-phosphate of ADP also interacts with the C4′ hydroxyl group of the bound pantothenate via a water molecule (labeled "W" in Figure 4), which is coordinated by the side chain of Asn9. This water molecule would

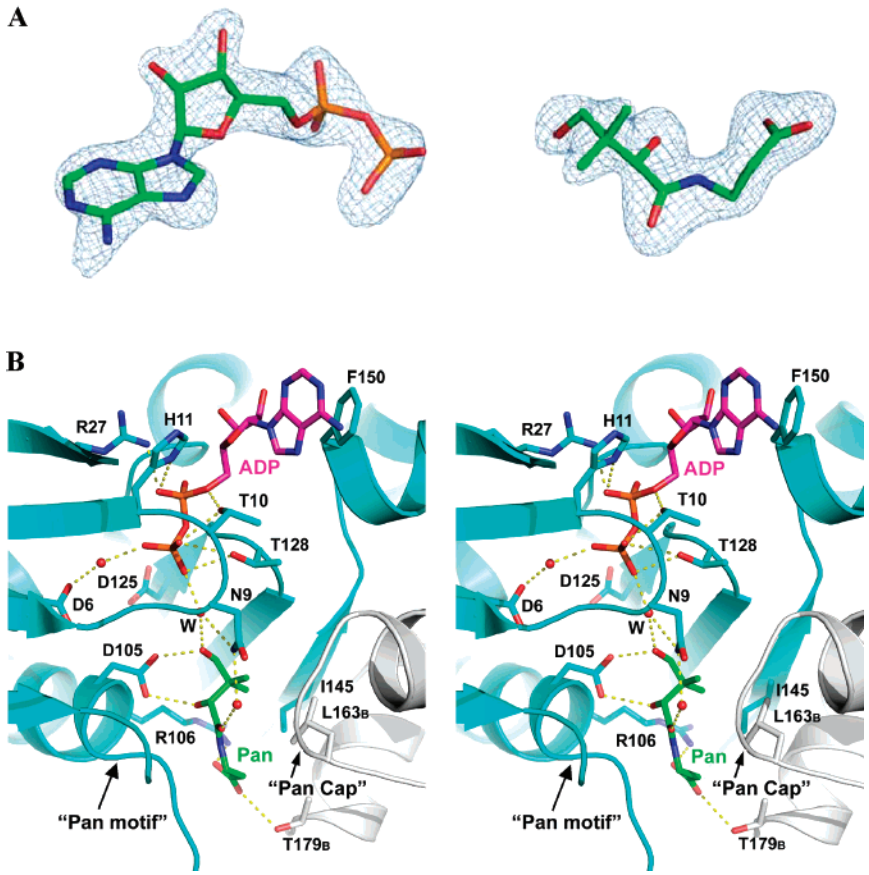

FIGURE 4: (A) $F_o - F_c$ omit map for ADP and Pan in *Tm*PanK-III ternary complex, contoured at 3.5σ. (B) Stereoview of pantothenate and ATP binding sites in *Tm*PanK-III. Pantothenate molecule (Pan) is colored green and ADP magenta. The two monomers in *Tm*PanK-III dimer are colored cyan and gray, respectively. Protein side chains that interact with substrates are drawn as sticks. Active site water molecules are shown as small red spheres. Hydrogen bonds are represented by dotted lines. Structural elements corresponding to "Pan cap" and "Pan motif" are indicated.

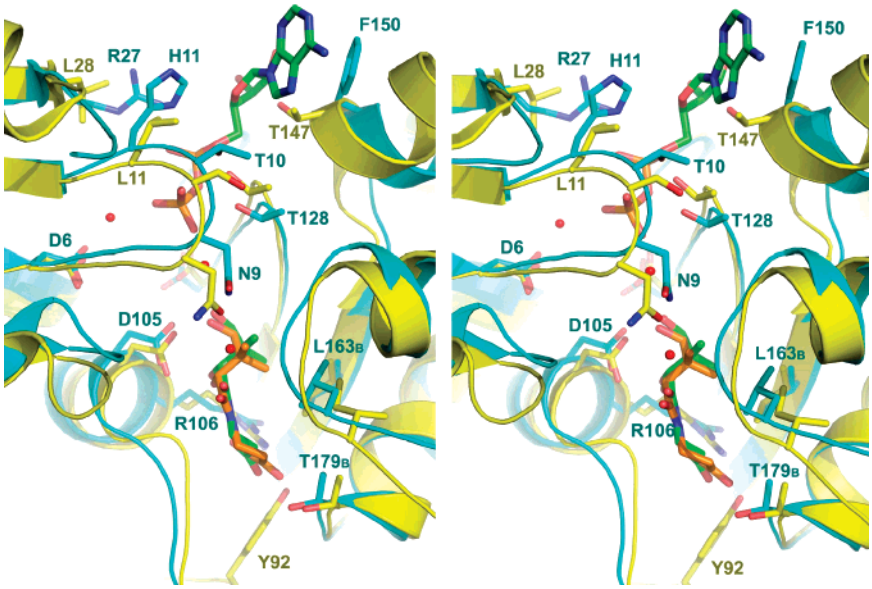

FIGURE 5: Superposition of the substrate binding sites of *Tm*PanK-III (cyan) and *Pa*PanK-III (yellow). The pantothenate and ADP bound to *Tm*PanK-III are shown in stick representation with carbon atoms colored in green. The pantothenate bound to *Pa*PanK-III is shown with carbon atoms colored in orange.

partially overlap with the γ-phosphate if an ATP molecule is to be bound in the same position as the ADP. It is likely that Asn9 directly interacts with the transferring γ-phosphate of ATP and thus plays an important role in catalysis. Mutation of the corresponding Asn residue to Ala in the *P. aeruginosa* enzyme resulted in a decrease of enzyme activity by 100-fold, supporting its important role in either substrate binding or catalysis (*22*). There are essentially no specific interactions observed between the enzyme and the ribose group of ADP (Figure 4B). The interaction between the enzyme and the adenine ring of ADP is also very limited, involving primarily a weak stacking interaction with the side

chain of Phe150. The ATP binding pocket of *Tm*PanK-III opens up considerably to the solvent and does not support tight interactions with the adenosyl moiety of ATP (Figures 3A and 4B).

The observed nucleotide binding mode in PanK-III provides a structural explanation for the low binding affinity for ATP. It also explains why PanK-III enzymes do not discriminate strongly among various NTPs or dNTPs, and possibly why purine nucleotides are better phosphate donors than pyrimidine nucleotides. It is possible that, since adenine and guanine bases have bigger surface areas than the pyrimidine bases, they may form slightly stronger van der Waals interactions with the enzyme and thus may have a somewhat higher binding affinity. Since there are few specific direct interactions between PanK-III and the ribose moiety of the bound nucleotide, PanK-III is nearly equally as active when using dNTPs compared to NTPs as phosphoryl donors (*22*).

The *Tm*PanK-III·ADP complex is the only nucleotide-complexed PanK-III structure available at present. Superposition of *Tm*PanK-III·Pan·ADP structure with that of PanK-III from *P. aeruginosa* and *B. anthracis* brings ADP into the active sites of these enzymes without any serious steric clashes, thus offering a model of ADP binding in PanK-III from different species (Figure 5). In this model, Thr10 and Thr128 of *Tm*PanK-III, corresponding to Ser10 and Thr124 of *Pa*PanK-III, and Thr10 and Thr132 of *Ba*PanK-III, respectively, are well conserved in all three enzymes (Figure 3B). The His11 and Arg27 residues of *Tm*PanK-III that are involved in ATP binding are also well conserved in *B. anthracis* and many other PanK-III enzymes (Figure 3B). However, these residues are respectively changed to Leu11 and Leu28 in *Pa*PanK-III, which are no longer able to form the same specific interactions with ATP. Therefore, there appears to be some variation in the ATP binding sites among PanK-III enzymes from different species. However, these variations do not appear to alter the enzymes' low overall affinity toward ATP, since all the PanK-III enzymes characterized to date have similar high K_m values (in the mM range).

TmPanK-III Product Complex Structure and Catalytic Mechanism of PanK-III. We have determined the structure of *Tm*PanK-III complexed with its product phosphopantothenate (P-Pan, Figure 6). The less than optimal density for the terminal phosphate of the bound product indicates partial occupancy of this phosphate group, probably due to degradation of the original product stock solution upon storage. Subsequent ES-MS analysis of the stock solution confirmed the presence of significant amounts of pantothenate in addition to the expected P-Pan. In this complex structure the side chain of Asn9, previously interacting with a water molecule bridging pantothenate C4′ hydroxyl and ADP β-phosphate in the *Tm*PanK-III·ADP·Pan ternary complex structure (Figure 4B), is now hydrogen bonded to the phosphate group of P-Pan. When an ADP molecule is modeled in this product complex according to the *Tm*PanK-III·Pan·ADP structure to generate a ternary product complex model, the distance between one of the oxygen atoms of the ADP β-phosphate and the phosphorus of P-Pan is only ~3.0 Å and it is collinear with the P−O4′ bond of P-Pan (Figure 6). This active site configuration is consistent with a mechanism in which the phosphoryl transfer proceeds via a

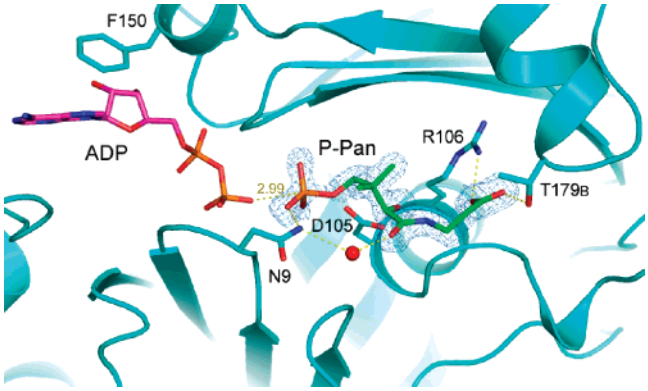

FIGURE 6: Interactions between *Tm*PanK-III and product phosphopantothenate (P-Pan) in the *Tm*PanK-III·P-Pan binary complex. The $F_o - F_c$ omit map for P-Pan, contoured at 2.5σ, is shown. The ADP molecule was modeled according to the *Tm*PanK-III·Pan·ADP ternary complex structure. Hydrogen bonds are represented as dotted lines.

nucleophilic attack by the C4′ hydroxyl group of pantothenate on the γ-phosphorus of ATP, followed by direct in-line transfer of the terminal phosphate to C4′ hydroxyl. The short distance between the two terminal phosphoryl groups (4.47 Å) would suggest a large degree of associative character in the phosphoryl transfer reaction catalyzed by PanK-III (*47*, *48*). Two Asp residues of the PHOSPHATE 1 and PHOSPHATE 2 motifs, Asp6 and Asp125, have been proposed to coordinate the catalytic Mg^{2+} and/or K^+/NH_4^+ ions that interact with ATP's β- and γ-phosphates and stabilize the reaction intermediate. Additionally the highly conserved Asp105 residue is ideally positioned to act as the catalytic base in activating the C4′ hydroxyl group of pantothenate for nucleophilic attack on ATP γ-phosphate (Figure 4). However, results from mutagenesis analysis of this residue in the PanK-III enzymes from *H. pylori* and *P. aeruginosa* have not been conclusive in confirming this role. While a conservative mutation of this aspartate residue to Asn or Glu reduced the activity of *Hp*PanK-III to <5% of that of the wild-type enzyme (*20*), an Asp to Ala mutation in *Pa*PanK-III retained as much as 20% of the wild-type enzyme activity (*22*). It is clear that this Asp residue at least plays a role in substrate binding as it coordinates the phosphoryl receptor group in the active site of the enzyme. Further investigations will be needed to determine whether and to what extent it is also involved in chemical catalysis.

Comparison of PanK-III and PanK-II Enzymes. Although type II and type III PanK proteins both adopt the same overall fold and belong to the same ASHKA superfamily, they share only limited sequence identity (~13%) and have distinct kinetic properties and substrate preferences (*7*, *21*, *22*, *25*). Structural comparison of PanK-III with the recently published PanK-II structures from both *S. aureus* and human sources reveals that, while the overall fold and key catalytic residues are conserved, the conformations of the substrate binding sites for both ATP and pantothenate are significantly different in these two distantly related PanKs. First, a superposition of the AMNPNP bound *Sa*PanK-II (*22*) and the ADP bound *Tm*PanK-III structures shows that the positioning of the bound nucleotide in the two enzymes is very different, especially in the adenosine portion (Figure 7A). Different sets of protein residues are involved in the interactions with the adenosyl moiety of the nucleotide in PanK-II and PanK-

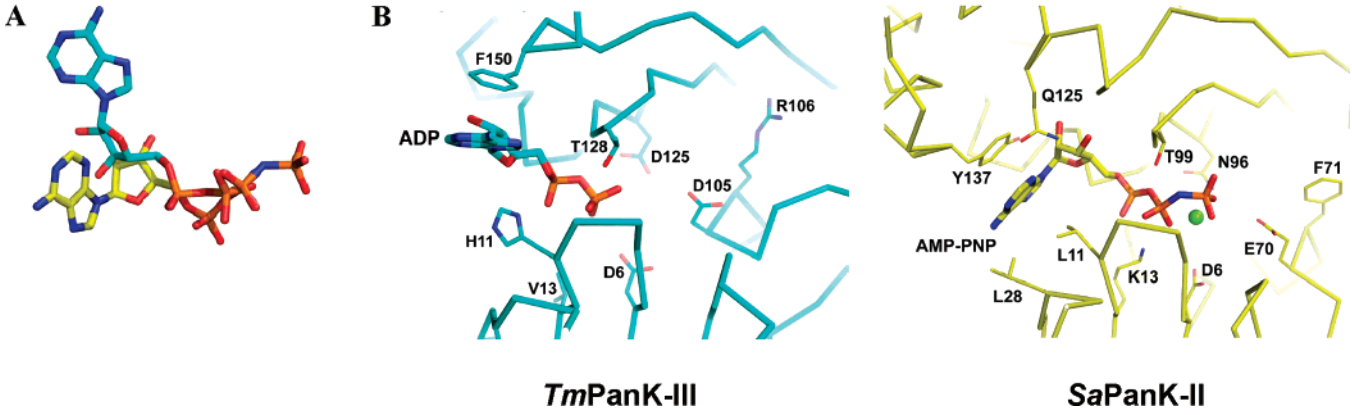

FIGURE 7: Comparison of nucleotide binding in PanK-III and PanK-II. (A) Superposition of *Tm*PanK-III bound ADP (cyan) and *Sa*PanK-II bound AMPPNP (yellow). This superposition is achieved by overlaying the conserved active site residues of the two enzymes. (B) A side-by-side view of the nucleotide binding site of PanK-III from *Thermotoga maritima* (left) and PanK-II from *Staphylococcus aureus* (right). The proteins are shown as C_α traces. The Mg^{2+} ion is shown as a green sphere. Selected protein side chains are also shown.

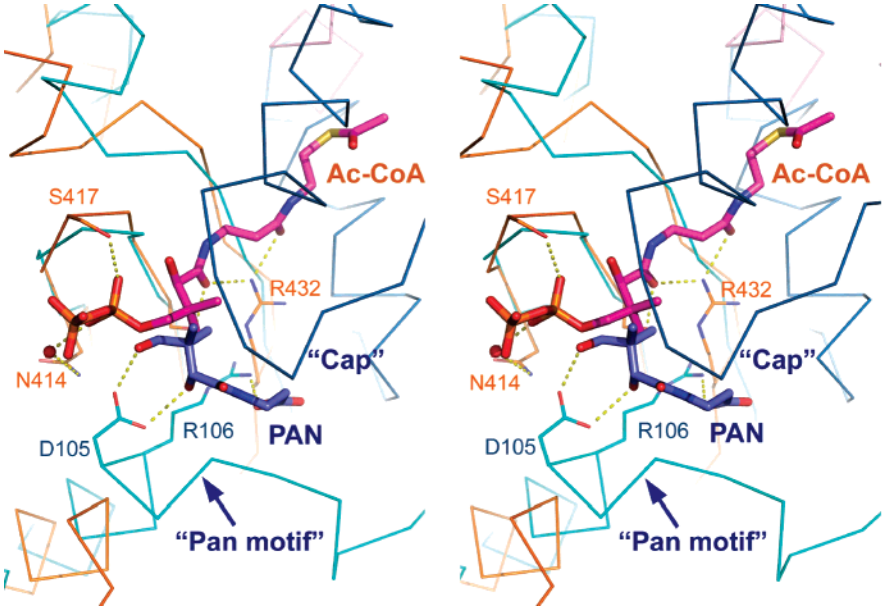

FIGURE 8: Stereoview of the superposition of the pantothenate binding sites in *Tm*PanK-III (light and dark blue) and human PANK1 (orange). Only C_α traces of proteins are shown. Pantothenate (blue) bound to *Tm*PanK-III and acetyl-CoA (magenta) bound to *hs*PANK1 are show as thick sticks. The adenosine moiety of the acetyl-CoA molecule is not present in the PDB coordinates (code 2i7n), and is presumably disordered in the structure. Residues 466−512 of *hs*PANK1 are removed for clarity. Selected protein side chains are shown as thin sticks, while dotted lines represent hydrogen bonds. An active site water molecule in *hs*PANK1 is shown as a red sphere.

III (Figure 7B). On the other hand, the β- and γ-phosphates of the bound nucleotides are likely to occupy similar positions and interact with the same conserved set of protein residues such as those in the PHOSPHATE 1 (containing Asp6, Asn9 and Thr10, using *Tm*PanK-III numbering) and PHOSPHATE 2 (containing Asp125 and Thr128) motifs either directly or indirectly through solvent molecules. In contrast to PanK-III, where there is little specific interaction between the enzyme and the adenosine moiety of the nucleotide, the adenine ring of AMPPNP bound to *Sa*PanK-II is sandwiched between the side chains of Tyr137 and Leu11 (Figure 7B, right panel). There are also additional specific hydrogen bonds and hydrophobic interactions between *Sa*PanK-II and the nucleotide that are not present in PanK-III. These include the interactions of the main chain carbonyl of Gly121 with the O2′ hydroxyl, of Gln125 and Leu28 with the adenine base (Figure 7B), and of Lys13 (corresponding to Val13 in *Tm*PanK-III) with the α- and β-phosphates of the nucleotide. Overall, type II PanK, as represented here by *Sa*PanK, has a better suited ATP binding pocket compared to type III PanK, and forms more extensive hydrogen bond and van der Waals interactions with the nucleotide.

At present, a complex structure of a type II PanK with its pantothenate substrate has not been reported. In the absence of an experimentally determined PanK-II·Pan complex structure, the recent structures of two human PanK isoforms (PANK1 and PANK3) complexed with a physiological feedback inhibitor acetyl-CoA (pdb code 2i7n and 2i7p) (*29*) may act as a model for pantothenate binding in PanK-II, assuming that the Pan substrate would occupy the same position as that of the pantothenate moiety of acetyl-CoA (Figure 8). This mode of pantothenate binding in human PanK is drastically different from that observed in PanK-III. When the active site residues of *Tm*PanK-III and human PanK-II are superimposed, the pantothenate moieties in the two complex structures overlap only at the position of the C4′ hydroxyl groups, with the rest of the molecule orientated very differently and interacting with an entirely different set

of protein residues (Figure 8). Notably the Pan binding sites in both PanK-II and PanK-III are located near the dimer interface. Due to the different structures of the insertion elements which comprise a large portion of the dimer interface in both PanK-II and PanK-III, the relative arrangement of two monomers in the dimer are very different for the two enzymes, resulting in distinct and mutually exclusive Pan-binding pockets. The PanK-II dimer interface leaves a long and solvent accessible channel that can accommodate pantothenate and the longer *N*-substituted pantothenamides as substrates. It is also able to bind CoA and acetyl-CoA as inhibitors as demonstrated by the complex structures of human PanK-II isoforms with acetyl-CoA (*29*). In contrast, the dimer interface in PanK-III generates a much smaller and enclosed binding pocket that is not able to accommodate either *N*-alkylpantothenamides or CoA and its analogues.

In conclusion, we would like to emphasize that although pantothenamides have been shown to effectively inhibit the growth of *E. coli* and *S. aureus*, two organisms harboring type I and type II PanKs, respectively (*7*, *18*), this inhibition is strictly due to the *in vivo* conversion of these compounds by the target organism's CoA biosynthetic machinery (including the PanK enzyme) into corresponding CoA analogues. These analogues subsequently act as antimetabolites, interfering with the function of CoA-dependent enzymes (*6*, *21*). Furthermore, it has been shown that pantothenamides do not have any inhibitory effects on *P. aeruginosa*, which contains only a type III PanK (*22*). The potential application of pantothenamide-type antibiotics therefore seems to be limited to organisms that contain only the promiscuous PanK-I or PanK-II enzymes which will act on these compounds as substrates. To date no compound—apart from the natural feedback inhibitors of PanKs—has been reported to directly inhibit the kinase activity of a PanK enzyme. Clearly, alternative strategies are needed to develop new types of specific inhibitors that target PanK enzymes in general, and the type III PanKs that occur in a wide range of pathogenic bacteria in particular. The detailed enzyme−substrate interactions and the drastically different substrate binding modes of PanK-II and PanK-III enzymes that have been revealed in this study may facilitate the design of such *bona fide* PanK inhibitors.

ACKNOWLEDGMENT

We are grateful to Meg Phillips for advice on enzyme kinetic experiments and critical reading of the manuscript, Diana Tomchick for help with synchrotron data collection, David Chuang and Scott Tso for help with ITC assays, and Nick Grishin for many enlightening discussions.

REFERENCES

1. Jackowski, S. (1996) in *Escherichia coli and Salmonella: cellular and molecular biology* (Neidhardt, F. C., Curtiss, R., Gross, C. A., Ingraham, J. L., Lin, E. C. C., Low, K. B., Magasanik, B. R., W., Riley, M., Schaechter, M., and Umbarger, H. E., Eds.) pp 687−694, ASM Press, Washington, D.C.
2. Begley, T. P., Kinsland, C., and Strauss, E. (2001) The biosynthesis of coenzyme A in bacteria, *Vitam. Horm. 61*, 157−171.
3. Leonardi, R., Zhang, Y. M., Rock, C. O., and Jackowski, S. (2005) Coenzyme A: back in action, *Prog. Lipid Res. 44*, 125−153.
4. Becker, D., Selbach, M., Rollenhagen, C., Ballmaier, M., Meyer, T. F., Mann, M., and Bumann, D. (2006) Robust *Salmonella* metabolism limits possibilities for new antimicrobials, *Nature 440*, 303−307.
5. Gerdes, S. Y., Scholle, M. D., D'Souza, M., Bernal, A., Baev, M. V., Farrell, M., Kurnasov, O. V., Daugherty, M. D., Mseeh, F., Polanuyer, B. M., Campbell, J. W., Anantha, S., Shatalin, K. Y., Chowdhury, S. A., Fonstein, M. Y., and Osterman, A. L. (2002) From genetic footprinting to antimicrobial drug targets: examples in cofactor biosynthetic pathways, *J. Bacteriol. 184*, 4555−4572.
6. Strauss, E., and Begley, T. P. (2002) The antibiotic activity of N-pentylpantothenamide results from its conversion to ethyldethiacoenzyme A, a coenzyme A antimetabolite, *J. Biol. Chem. 277*, 48205−48209.
7. Choudhry, A. E., Mandichak, T. L., Broskey, J. P., Egolf, R. W., Kinsland, C., Begley, T. P., Seefeld, M. A., Ku, T. W., Brown, J. R., Zalacain, M., and Ratnam, K. (2003) Inhibitors of pantothenate kinase: novel antibiotics for staphylococcal infections, *Antimicrob. Agents Chemother. 47*, 2051−2055.
8. Virga, K. G., Zhang, Y. M., Leonardi, R., Ivey, R. A., Hevener, K., Park, H. W., Jackowski, S., Rock, C. O., and Lee, R. E. (2006) Structure-activity relationships and enzyme inhibition of pantothenamide-type pantothenate kinase inhibitors, *Bioorg. Med. Chem. 14*, 1007−1020.
9. Song, W. J., and Jackowski, S. (1992) Cloning, sequencing, and expression of the pantothenate kinase (coaA) gene of *Escherichia coli*, *J. Bacteriol. 174*, 6411−6417.
10. Song, W. J., and Jackowski, S. (1994) Kinetics and regulation of pantothenate kinase from *Escherichia coli*, *J. Biol. Chem. 269*, 27051−27058.
11. Calder, R. B., Williams, R. S., Ramaswamy, G., Rock, C. O., Campbell, E., Unkles, S. E., Kinghorn, J. R., and Jackowski, S. (1999) Cloning and characterization of a eukaryotic pantothenate kinase gene (panK) from *Aspergillus nidulans*, *J. Biol. Chem. 274*, 2014−2020.
12. Rock, C. O., Calder, R. B., Karim, M. A., and Jackowski, S. (2000) Pantothenate kinase regulation of the intracellular concentration of coenzyme A, *J. Biol. Chem. 275*, 1377−1383.
13. Rock, C. O., Karim, M. A., Zhang, Y. M., and Jackowski, S. (2002) The murine pantothenate kinase (Pank1) gene encodes two differentially regulated pantothenate kinase isozymes, *Gene 291*, 35−43.
14. Falk, K. L., and Guerra, D. J. (1993) Coenzyme A biosynthesis in plants: partial purification and characterization of pantothenate kinase from spinach, *Arch. Biochem. Biophys. 301*, 424−430.
15. Yun, M., Park, C. G., Kim, J. Y., Rock, C. O., Jackowski, S., and Park, H. W. (2000) Structural basis for the feedback regulation of *Escherichia coli* pantothenate kinase by coenzyme A, *J. Biol. Chem. 275*, 28093−28099.
16. Vallari, D. S., Jackowski, S., and Rock, C. O. (1987) Regulation of pantothenate kinase by coenzyme A and its thioesters, *J. Biol. Chem. 262*, 2468−2471.
17. Zhang, Y. M., Chohnan, S., Virga, K. G., Stevens, R. D., Ilkayeva, O. R., Wenner, B. R., Bain, J. R., Newgard, C. B., Lee, R. E., Rock, C. O., and Jackowski, S. (2007) Chemical knockout of pantothenate kinase reveals the metabolic and genetic program responsible for hepatic coenzyme A homeostasis, *Chem. Biol. 14*, 291−302.
18. Clifton, G., Bryant, S. R., and Skinner, C. G. (1970) N′-(substituted) pantothenamides, antimetabolites of pantothenic acid, *Arch. Biochem. Biophys. 137*, 523−528.
19. Nicely, N. I., Parsonage, D., Paige, C., Newton, G. L., Fahey, R. C., Leonardi, R., Jackowski, S., Mallett, T. C., and Claiborne, A. (2007) Structure of the type III pantothenate kinase from *Bacillus anthracis* at 2.0 A resolution: implications for coenzyme A-dependent redox biology, *Biochemistry 46*, 3234−3245.
20. Yang, K., Eyobo, Y., Brand, L. A., Martynowski, D., Tomchick, D., Strauss, E., and Zhang, H. (2006) Crystal structure of a type III pantothenate kinase: insight into the mechanism of an essential coenzyme A biosynthetic enzyme universally distributed in bacteria, *J. Bacteriol. 188*, 5532−5540.
21. Leonardi, R., Chohnan, S., Zhang, Y. M., Virga, K. G., Lee, R. E., Rock, C. O., and Jackowski, S. (2005) A pantothenate kinase from *Staphylococcus aureus* refractory to feedback regulation by coenzyme A, *J. Biol. Chem. 280*, 3314−3322.
22. Hong, B. S., Yun, M. K., Zhang, Y. M., Chohnan, S., Rock, C. O., White, S. W., Jackowski, S., Park, H. W., and Leonardi, R. (2006) Prokaryotic type II and type III pantothenate kinases: The same monomer fold creates dimers with distinct catalytic properties, *Structure 14*, 1251−1261.
23. delCardayre, S. B., Stock, K. P., Newton, G. L., Fahey, R. C., and Davies, J. E. (1998) Coenzyme A disulfide reductase, the primary low molecular weight disulfide reductase from *Staphy-*

lococcus aureus. Purification and characterization of the native enzyme, *J. Biol. Chem. 273*, 5744−5751.
24. Luba, J., Charrier, V., and Claiborne, A. (1999) Coenzyme A-disulfide reductase from *Staphylococcus aureus*: evidence for asymmetric behavior on interaction with pyridine nucleotides, *Biochemistry 38*, 2725−2737.
25. Brand, L. A., and Strauss, E. (2005) Characterization of a new pantothenate kinase isoform from *Helicobacter pylori*, *J. Biol. Chem. 280*, 20185−20188.
26. Yocum, R. R., and Patterson, T. A. (Dec 14, 2002) U.S. Patent 6,830,898.
27. Overbeek, R., Begley, T., Butler, R. M., Choudhuri, J. V., Chuang, H. Y., Cohoon, M., de Crecy-Lagard, V., Diaz, N., Disz, T., Edwards, R., Fonstein, M., Frank, E. D., Gerdes, S., Glass, E. M., Goesmann, A., Hanson, A., Iwata-Reuyl, D., Jensen, R., Jamshidi, N., Krause, L., Kubal, M., Larsen, N., Linke, B., McHardy, A. C., Meyer, F., Neuweger, H., Olsen, G., Olson, R., Osterman, A., Portnoy, V., Pusch, G. D., Rodionov, D. A., Ruckert, C., Steiner, J., Stevens, R., Thiele, I., Vassieva, O., Ye, Y., Zagnitko, O., and Vonstein, V. (2005) The subsystems approach to genome annotation and its use in the project to annotate 1000 genomes, *Nucleic Acids Res. 33*, 5691−5702.
28. Cheek, S., Zhang, H., and Grishin, N. V. (2002) Sequence and structure classification of kinases, *J. Mol. Biol. 320*, 855−881.
29. Hong, B. S., Senisterra, G., Rabeh, W. M., Vedadi, M., Leonardi, R., Zhang, Y. M., Rock, C. O., Jackowski, S., and Park, H. W. (2007) Crystal structures of human pantothenate kinases: Insights into allosteric regulation and mutations linked to neurodegeneration disorder, *J. Biol. Chem. 282*, 27984−27993.
30. Cheek, S., Ginalski, K., Zhang, H., and Grishin, N. V. (2005) A comprehensive update of the sequence and structure classification of kinases, *BMC Struct. Biol. 5*, 6.
31. Bork, P., Sander, C., and Valencia, A. (1992) An ATPase domain common to prokaryotic cell cycle proteins, sugar kinases, actin, and hsp70 heat shock proteins, *Proc. Natl. Acad. Sci. U.S.A. 89*, 7290−7294.
32. Bradford, M. M. (1976) A rapid and sensitive method for the quantitation of microgram quantities of protein utilizing the principle of protein-dye binding, *Anal. Biochem. 72*, 248−254.
33. Strauss, E., Kinsland, C., Ge, Y., McLafferty, F. W., and Begley, T. P. (2001) Phosphopantothenoylcysteine synthetase from *Escherichia coli*. Identification and characterization of the last unidentified coenzyme A biosynthetic enzyme in bacteria, *J. Biol. Chem. 276*, 13513−13516.
34. Strauss, E., Zhai, H., Brand, L. A., McLafferty, F. W., and Begley, T. P. (2004) Mechanistic studies on phosphopantothenoylcysteine decarboxylase: trapping of an enethiolate intermediate with a mechanism-based inactivating agent, *Biochemistry 43*, 15520−15533.
35. Otwinowski, Z., and Minor, W. (1997) Processing of X-ray diffraction data collected in oscillation mode, *Methods Enzymol. 276*, 307−326.
36. Vagin, A., and Teplyakov, A. (1997) MOLREP: an Automated Program for Molecular Replacement, *J. Appl. Crystallogr. 30*, 1022−1025.
37. Murshudov, G. N., Vagin, A. A., and Dodson, E. J. (1997) Refinement of macromolecular structures by the maximum-likelihood method, *Acta Crystallogr., Sect. D: Biol. Crystallogr. 53*, 240−255.
38. Collaborative Computational Project Number 4. (1994) The CCP4 suite: programs for protein crystallography, *Acta Crystallogr., Sect. D: Biol. Crystallogr. 50*, 760−763.
39. Emsley, P., and Cowtan, K. (2004) Coot: model-building tools for molecular graphics, *Acta Crystallogr., Sect. D: Biol. Crystallogr. 60*, 2126−2132.
40. Laskowski, R. A., MacArthur, M. W., Moss, D. S., and Thornton, J. M. (1993) PROCHECK: A program to check the stereochemical quality of protein structures, *J. Appl. Crystallogr. 26*, 283−291.
41. DeLano, W. L. (2002) in www.pymol.org.
42. Berman, H. M., Westbrook, J., Feng, Z., Gilliland, G., Bhat, T. N., Weissig, H., Shindyalov, I. N., and Bourne, P. E. (2000) The Protein Data Bank, *Nucleic Acids Res. 28*, 235−242.
43. Viola, R. E., Raushel, F. M., Rendina, A. R., and Cleland, W. W. (1982) Substrate synergism and the kinetic mechanism of yeast hexokinase, *Biochemistry 21*, 1295−1302.
44. Anderson, C. M., Stenkamp, R. E., McDonald, R. C., and Steitz, T. A. (1978) A refined model of the sugar binding site of yeast hexokinase B, *J. Mol. Biol. 123*, 207−219.
45. Aleshin, A. E., Kirby, C., Liu, X., Bourenkov, G. P., Bartunik, H. D., Fromm, H. J., and Honzatko, R. B. (2000) Crystal structures of mutant monomeric hexokinase I reveal multiple ADP binding sites and conformational changes relevant to allosteric regulation, *J. Mol. Biol. 296*, 1001−1015.
46. Hurley, J. H. (1996) The sugar kinase/heat shock protein 70/actin superfamily: implications of conserved structure for mechanism, *Annu. Rev. Biophys. Biomol. Struct. 25*, 137−162.
47. Mildvan, A. S., and Fry, D. C. (1987) NMR studies of the mechanism of enzyme action, *Adv. Enzymol. Relat. Areas Mol. Biol. 59*, 241−313.
48. Matte, A., Tari, L. W., and Delbaere, L. T. (1998) How do kinases transfer phosphoryl groups, *Structure 6*, 413−419.

BI7018578